Environmental Science: Atmospheres

ROYAL SOCIETY OF CHEMISTRY

PAPER

View Article Online
View Journal | View Issue

Cite this: *Environ. Sci.: Atmos.*, 2023, **3**, 182

Changes in CCN activity of ship exhaust particles induced by fuel sulfur content reduction and wet scrubbing†

Luis F. E. d. Santos, *[a] Kent Salo,[b] Xiangrui Kong,[a] Jun Noda,[c] Thomas B. Kristensen,‡[d] Takuji Ohigashi[e] and Erik S. Thomson *[a]

Maritime transport remains a large source of airborne pollutants, including exhaust particles that can act as cloud condensation nuclei (CCN). While primary diesel engine exhaust particles are generally considered hydrophobic, international regulations targeting a reduction of particulate emissions from ships may have secondary effects, and therefore influence how exhaust interacts within the atmosphere. The effect of international fuel sulfur content (FSC) regulations on the cloud forming abilities of exhaust particles was investigated using a marine test engine operating on compliant low FSC fuels, non-compliant high FSC distillate fuels and in conjunction with a marine wet scrubber (fresh- and seawater). Particle sizing and liquid droplet activation measurements reveal that compliance measures can have opposing effects on the CCN activity of exhaust particles. For a non-compliant, high FSC fuel, wet scrubbing leads to an increase in CCN activity but not to significant increases in CCN emission factors. However, switching to low FSC fuels resulted in emissions of highly hydrophobic particles, causing a significant reduction in CCN activity resulting in smaller CCN emission factors by at least one order of magnitude. Our observations are supported by chemical analysis of exhaust particles using scanning transmission X-ray microscopy and near edge X-ray absorption fine structure (STXM/NEXAFS) spectra. Potential implications of effects on ship exhaust particles for cloud and climate interactions due to different compliance measures are discussed.

Received 8th July 2022
Accepted 3rd November 2022

DOI: 10.1039/d2ea00081d

rsc.li/esatmospheres

Environmental significance

International marine fuel regulations are aimed at reducing emissions of airborne pollutants from the shipping sector. Using either low sulfur content fuels or alternatively high sulfur content fuels with exhaust wet scrubbers are two paths to achieving compliance that have been shown to result in unintended secondary effects on particulate matter. Here, we specifically study how these compliance alternatives affect cloud condensation nuclei (CCN) activity of fresh exhaust particles. Whereas fuel sulfur content reductions are observed to lower CCN emissions, wet scrubbing affects chemical mixing states and leads to increased emissions of more hygroscopic exhaust particles. These findings may have important implications for cloud processes and climatic feedbacks. This is of particular interest, as shipping activity is projected to increase in the Arctic, a region already subject to unprecedented anthropogenic induced climate feedbacks.

1 Introduction

The maritime shipping sector is a major contributor of anthropogenic air pollutants, such as particulate matter (PM).[1] Ship exhaust particles are primarily formed from incomplete combustion but may also be formed from secondary gas-phase precursors. They usually consist of carbon-containing aerosol, *e.g.* black carbon (BC), and may include other inorganic components,[2,3] such as sulfates and other sulfur-containing species, which are highly dependent on the sulfur content of the fuel (FSC; fuel sulfur content).[4] Physicochemical properties of ship exhaust particles are generally determined by multiple factors, such as the fuel type consumed,[5–8] engine type and load[2,5,7] and consumption and type of lubricating oil.[8,9] While particle mass emissions from ships can be dominated by large, primary particles of several μm,[10] particle number (PN) emissions are generally dominated by fine particles around 100 nm in diameter. Ultrafine particulate (<100 nm) can enter the human body through the respiratory system and cause *e.g.* cardiovascular diseases.[11] Previous studies have estimated that

[a]*Atmospheric Science, Department of Chemistry and Molecular Biology, University of Gothenburg, 41296 Gothenburg, Sweden. E-mail: luis.santos@cmb.gu.se; erik.thomson@chem.gu.se*

[b]*Maritime Studies, Department of Mechanics and Maritime Sciences, Chalmers University of Technology, 41756, Gothenburg, Sweden*

[c]*School of Veterinary Medicine, Rakuno Gakuen University, Ebetsu, Hokkaido 069-8501, Japan*

[d]*Department of Physics, Lund University, 22100, Lund, Sweden*

[e]*UVSOR Synchrotron, Institute for Molecular Science, 444-8585 Okazaki, Japan*

† Electronic supplementary information (ESI) available. See DOI: https://doi.org/10.1039/d2ea00081d

‡ Now at: Force Technology, 2605 Brøndby, Denmark.

shipping contributes ~60 000 premature deaths per year[12] and that as many as 45 000 premature mortalities could be prevented by lowering the FSC of marine fuels.[13]

Particulate emissions from ships also impact the climate system by either directly interacting with solar radiation, through absorption and scattering, or by acting as cloud nuclei, affecting microphysical cloud processes and hence, their lifetimes and radiative properties.[14] Marine vessels can be a significant source of localized cloud condensation nuclei (CCN) emissions which is of particular interest in remote marine environments, where aerosol particle background concentrations are low.[5,15–19] Diesel engine exhaust particles, specifically BC, are generally considered hydrophobic and thus, lead to a net warming effect due to absorption of radiation.[20] Studies measuring CCN emissions from ships found, for example, reductions in emissions when switching to lower FSC fuels, which can be attributed to smaller fractions of sulfates in the particulate as well as a general shift towards emissions of smaller particles.[5,16,19] Moreover, the ability of ship exhaust particles to act as CCN may change due to co-emission and condensation of other (in)organic compounds that undergo photochemical transformations during particles' atmospheric residence time. This can affect chemical compositions, morphologies and consequently, CCN activities.[20–23] The extent to which aerosol perturbations caused by ship emissions can alter cloud properties and what implications this has for the net climate effect on global and regional scales is debated in literature and uncertainties persist.[24–29]

Over the past decades the International Maritime Organization (IMO) has introduced regulations limiting the maximum allowed FSC in marine fuels, aiming to reduce emissions of sulfur oxides (SO_x) and PM from ships. In January 2020, the global limit was reduced from 3.5% to 0.5% (by mass). Stricter limits are enforced in sulfur emission control areas (SECAs), where the FSC has been limited to 0.1% since 2015. An alternative to low FSC fuels, is the on-board installation of exhaust gas aftertreatment systems, particularly wet scrubber (WS) systems, which allow ships to run on high FSC fuels as long as they meet certain criteria regarding gaseous exhaust emissions.[30,31] Wet scrubbing, which has been employed in industrial plants for a longer period of time compared to the shipping sector, removes SO_x by spraying sea- or freshwater (with added buffering agents) into the ship exhaust. The water droplets capture gaseous SO_x which is removed with the discharge water before the exhaust gas is emitted into the atmosphere.[32,33] As a side-effect, WS can also remove PM from the exhaust to a certain extent. Whereas the SO_x removal efficiency of such WS systems is undisputed, studies investigating PM removal from scrubbers installed on-board ships show large variability in removal efficiency owing to differences in WS designs, engines and fuels used, as well as sampling methods. Wet scrubbing related PM emission reductions from ships range from no significant reduction at high engine loads to 75% of total PM.[34–38] Moreover, wet scrubbing has been shown to have secondary effects on PM emitted from ships affecting mixing states, morphologies and densities.[39,40] As a consequence, while reducing PM emissions, this can make generally hydrophobic diesel engine exhaust particles more hygroscopic and thus, have a climate cooling effect by increasing direct aerosol radiation scattering as well as indirect cloud–aerosol interactions. A recent survey of global ship-tracks by Yuan *et al.*[41] shows, for example, that the FSC limits implemented in 2015 caused strong reductions in ship-track density in SECAs, due to reduced emissions of sulfur and general shifts in shipping routes. Moreover, the authors find that global 2020 fuel standards led annual mean ship-track density to decrease by 50% or more compared to the climatological mean in major shipping lanes. However, FSC regulations appear to have opposing effects on microphysical properties of marine clouds within SECA and non-SECA regions.[41]

In this study a marine test-bed engine was used to characterize how international regulations targeting emission reductions of airborne pollutants from the shipping sector, *i.e.* usage of low FSC fuels and wet scrubbers, alter CCN formation abilities of submicron exhaust particles. Here we present on-line measurements of CCN activities and off-line chemical analysis using scanning transmission X-ray microscopy (STXM) to unravel physical and chemical reasons for the observed behavioural changes. Both compliant (FSC < 0.1%) as well as non-compliant (FSC > 0.1%) marine distillate fuels were used. A laboratory based WS was operated in conjunction with the non-compliant fuel.

2 Methods

Results presented in this study were obtained during measurement campaigns performed between 2019 and 2021. Data from on-line gas and aerosol instrumentation were measured during engine experiments at the Chalmers University of Technology's Marine Engine Laboratory in Gothenburg, Sweden. The instrumental setup used at the engine laboratory is illustrated in Fig. 1. Given the large number of acronyms associated with aerosol instrumentation, fuels, and analysis techniques we provide a list of acronyms within the ESI (see Table S1†). Off-line analyses examining chemical properties of exhaust particles were conducted at the BL4U beamline at the UVSOR Synchrotron Facility in Okazaki, Japan, and the SoftiMAX beamline at MAX IV Laboratory in Lund, Sweden.

2.1 Chalmers Marine Engine Laboratory

The Marine Engine Laboratory is equipped with a four-stroke, common-rail Volvo Penta D3-110 marine diesel engine. During the measurement campaigns it was operated at an engine load of 32 ± 1%. Equal combustion conditions across all experiments were ensured by continuously monitoring engine parameters and gaseous emissions as well as using the same types and batches of distillate fuels. In total, three different marine distillate fuels were used to investigate the effects of IMO FSC regulations on physicochemical properties of the exhaust particles. Detailed information on fuel properties can be found in Table 1. The high FSC fuel used in this study was heavy gas oil (HGO; FSC = 0.86%). It was not possible to operate the engine with higher viscosity, residual fuel oils such as HFO,

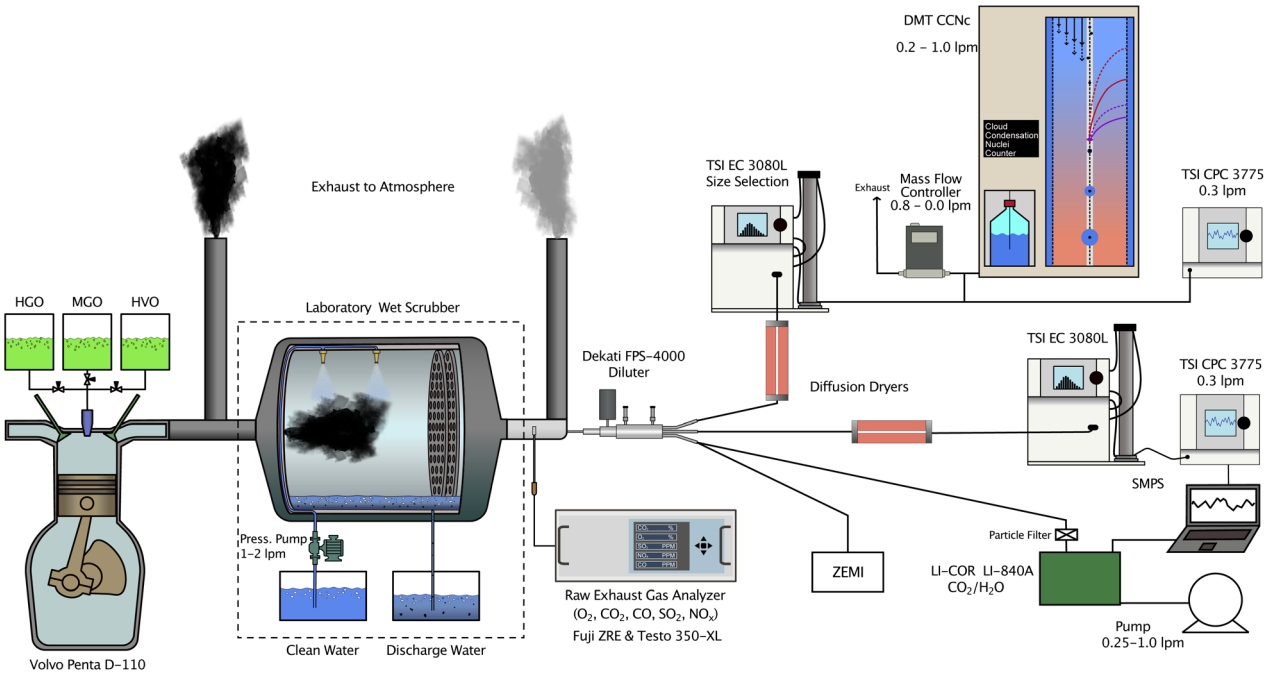

Fig. 1 An experimental setup schematic comprising instrumentation used in 2019 and 2020. The dashed box around the laboratory wet scrubber (WS) signifies that it was bypassed except for actual WS experiments when exhaust gas was directed through it. WS experiments were performed using the high FSC fuel HGO. See Section 2 for more details.

although HFO fuels are more representative of marine fuels used on-board large container ships. Within this study HGO represents the class of high FSC marine fuels which do not meet IMO FSC compliance on global as well as SECA levels. The low FSC fuels (FSC < 0.03%) reach IMO FSC compliance both on global and SECA levels. Marine gas oil (MGO) is commonly used for medium- and high-speed engines within the shipping sector whereas hydrotreated vegetable oil (HVO) is a distillate fuel made of renewable raw materials such as rapeseed oil. Compared to HGO and MGO, HVO has a significantly lower density as well as low aromatic content (0.2 vol%). The amount of metals within the samples was relatively low. All three fuels contain K whereas Cu was only detected in the HGO sample. All other analyzed metals were below detection limits.

Table 1 Chemical compositions and properties of the studied fuels; heavy gas oil (HGO; FSC = 0.86%), marine gas oil (MGO; FSC < 0.03%) and hydrotreated vegetable oil (HVO; FSC < 0.03%). Fuel samples were analyzed in 2019 and 2021 by Saybolt Sweden, Gothenburg

	HGO	MGO	HVO
Density at 15 °C [kg m^{-3}]	865.3	847.4	780.0
Heat of combustion [MJ kg^{-1}]			
Gross heat of combustion	45.02	45.60	46.57
Net heat of combustion	42.30	42.79	43.55
Carbon content [%]	86.4	86.5	85.2
Sulfur content [%]	0.86	<0.03	<0.03
Aromatic content [vol%]			
Total aromatics	27.4	23.6	0.2
Mono-aromatics	20.2	20.5	0.2
Di-aromatics	6.46	2.60	<0.1
Poly aromatics (Tri+)	0.71	0.43	<0.02
Additive and wear metals [mg kg^{-1}]			
Cu	1.81	<0.1	<0.1
K	0.4	0.27	0.25
Al, Ca, Cr, Fe, Pb, Ni, Na, V, Zi	<0.1	<0.1	<0.1

The WS used in this study was non-commercial and constructed at Chalmers University of Technology. It is designed to reduce SO_x emissions by spraying water droplets into the exhaust gas. During the measurements the total water flow rate distributed across all nozzles was controlled by a pressure pump and varied between 1.5 and 2 l min^{-1}. More information on the laboratory WS, including physical dimensions, is detailed in Santos *et al.*[40] During wet scrubbing experiments both freshwater, taken from Gothenburg's municipal water supply, and seawater were used. Seawater samples were either collected from surface water near the southern archipelago of Gothenburg or provided by University of Gothenburg's Kristineberg Marine Research Station north of Gothenburg. It was ensured that the wet scrubber was operated at SECA compliance levels, *i.e.* the ratio between emitted SO_2 in ppm and CO_2 in % is ≤4.1.[31] Further information regarding the SO_2 removal efficiency can be found in Santos *et al.*[40]

2.2 Gas and aerosol instrumentation

Emissions of gaseous compounds including O_2, CO_2, CO, NO_x and SO_2 were monitored in 1–5 second intervals using either a single-beam NDIR analyzer (Model ZRE, Fuji Electric Co., Ltd., Japan) or a Testo 350-XL flue gas analyzer (Testo SE & Co. KGaA, Germany). In all experiments a 2-stage fine particle sampler (FPS-

4000, Dekati Ltd., Finland) was used to dilute the exhaust gas before entering aerosol instrumentation. The dilution factor of both stages was controlled within the FPS unit. Dilution ratios during experiments were determined based on measured CO_2 ratios between raw and diluted exhaust. A LI-840A CO_2 analyzer (LICOR Inc., USA) was used to determine the CO_2 concentration in the diluted exhaust gas. During measurements involving the WS, IMO FSC regulation compliance was monitored according to the *IMO Guidelines for Exhaust Gas Cleaning Systems*.[31]

Particle size distributions (PSD) including statistical information, such as count median diameters (CMD) and geometric standard deviations (σ_g), used in this study are reproduced from Santos *et al.*[40] Herein, PSDs in the form of (bimodal) lognormal distributions represent average combustion conditions for the engine and fuels at an engine load of ≈32%. A scanning mobility particle sizer (SMPS; Electrostatic classifier, EC, Model 3080L, and condensation particle counter, CPC, Model 3075, TSI Inc., USA) covering a mobility diameter (d_{mo}) range of 15.1 nm to 661.2 nm was used to measure the PSDs. All PSDs were corrected for multiple charging artefacts and size-dependent diffusional losses within the instruments and the tubing. Moreover, number concentrations of individual size bins and the total particle population, were corrected for dilution factors. Particle number emission factors (EF_{PN}) can be calculated using the formula

$$EF_{PN} = \frac{Q_{exh} N_{PN}}{FC}, \quad (1)$$

where Q_{exh} is the exhaust gas flow in [$m^3\ h^{-1}$], which was calculated using a simplified model assuming all carbon in the fuel is converted to CO_2 during combustion,[40,42] N_{PN} is the particle number concentration in [$\#\ m^{-3}$] calculated by numerical integration of the PSDs, and FC is the fuel consumption in [$kg\ h^{-1}$]. Prior to entering any aerosol analysis instrumentation, diluted sample flow was dried using silica gel diffusion dryers.

2.3 CCN measurements and derivation of the hygroscopicity parameter κ

The ability of engine exhaust particles to act as CCN was investigated using a single column CCN counter (CCNc; CCNC-100, DMT). The growth chamber of the CCNc consists of a wetted column to which a stream-wise (increasing) temperature gradient (ΔT) is applied. The supersaturation (SS) achieved within the CCNc depends on the sample flow rate (Q) and ΔT and can be increased by either increasing Q or ΔT. The operating principle of the CCNc is described in detail elsewhere.[43,44] The CCNc was operated in Scanning Flow CCN Analysis (SFCA) mode as described by Moore and Nenes.[45] SFCA allows for continuous measurements of SS spectra by ramping the sample flow rate while keeping ΔT constant. The sample flow rate was increased from 0.2 to 1.0 l min^{-1} at a constant rate for 120 s. At 0.2 and 1.0 l min^{-1} the sample flow rates were kept constant for 30 s. A mass flow controller (MFC) operated in parallel with the CCNc maintained the total flow rate (Q_{CCNc} + Q_{MFC}) at 1.0 l min^{-1}. The usage of the CCNc under similar operating conditions has previously been studied by Wittbom *et al.*[22] and Kristensen *et al.*[46] Supersaturation spectra were measured at ΔT = 4, 10 and 18 °C, resulting in a SS range of 0.07–2.4%. Exhaust particles were size-selected at d_{mo} = 50, 90 and 150 nm using an EC (Model 3080L, TSI Inc., USA). A CPC (Model 3775, TSI Inc., USA) measured total particle number (condensation nuclei) concentrations (N_{CN}) parallel to the CCNc. These combined measurements allowed for determination of activated fractions. All CCN spectra were individually inspected and multiple charging artefacts were accounted for by identification of pre-activation plateaus. Critical supersaturations (SS_c; activation of 50% of the size-selected singly charged particle population into cloud droplets) were determined by fitting the measured activation curves to sigmoidal functions,[45]

$$\frac{N_{CCN}}{N_{CN}} = a_0 + \frac{a_1 - a_0}{1 + (Q_{CCNc}/Q_{50})^{-a_2}}, \quad (2)$$

where a_0, a_1, a_2 and Q_{50} are the minimum, maximum, slope, and inflection point respectively. Data were converted from Q_{50} to SS_c using linear fits derived from instrument calibrations (see ESI; Fig. S2†).

The resulting SS_c values were converted to the dimensionless hygroscopicity parameter (κ) using,

$$\kappa = \frac{4A^3}{27 d_{mo}{}^3 \ln^2(1 + SS_c/100\%)}, \quad \text{with } A = \frac{4\sigma_w M_w}{RT\rho_w}, \quad (3)$$

where SS_c is given in %, σ_w = 71.99 mN m^{-1} is the surface tension of water at 25 °C, M_w is the molar mass of water, R is the universal gas constant, T is the absolute temperature and ρ_w is the density of water at 25 °C (ρ_w = 0.997 g cm^{-3}).[47] The CCNc was calibrated during the campaign using $(NH_4)_2SO_4$ particles generated from an aerosol generator (3079A, TSI Inc., USA; see Fig. S2†).

2.4 Calculation of CCN emission factors

CCN emission factors (EF_{CCN}) were estimated in similar fashion to Kristensen *et al.*[46] Herein, a simple model is applied where κ values for d_{mo} between 50 nm and 150 nm were estimated using exponential fit functions (see ESI, eqn (S1)†). For d_{mo} smaller than 50 nm or larger than 150 nm the κ value of the respective threshold value was assumed. A more detailed description of this method is provided in the ESI.† Resulting size-dependent κ values are shown in Fig. S3.† Thereafter, κ values were converted into corresponding SS_c using eqn (3), which were used to calculate the activated fraction of a PSD at a given supersaturation. Case dependent PN concentrations from the 2020 campaign were used (Fig. 2).

EF_{CCN} were calculated in a similar fashion to eqn (1),

$$EF_{CCN} = \frac{Q_{exh} N_{CCN}(SS)}{FC}, \quad (4)$$

where N_{CCN}(SS) is the number concentration of CCN as a function of SS [$\#\ m^{-3}$].

2.5 Chemical characterization of exhaust particles using STXM/NEXAFS

The combination of scanning transmission X-ray microscopy (STXM) and near edge X-ray absorption fine structure (NEXAFS)

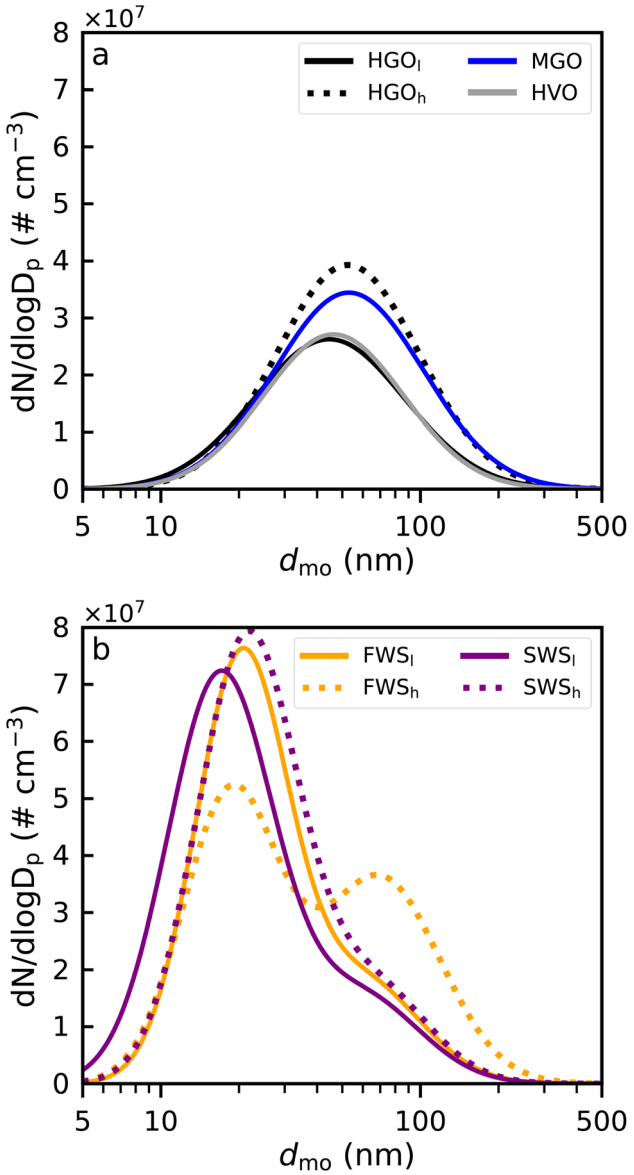

Fig. 2 Lognormal least squares fits representing particulate emissions for all five fuel and aftertreatment cases retrieved from measured particle size distributions (PSD). All PSDs have been corrected for diffusion losses and dilution factors.[40] (a) HGO, HVO and MGO designate exhaust particles produced from the combustion of the respective fuels, whereas (b) FWS and SWS indicate HGO combustion in conjunction with wet scrubbing using either sea- (SWS) or freshwater (FWS). In both WS cases bimodal lognormal distributions have been fitted to the data points. Variations in combustion conditions for HGO, FWS and SWS, characterized by changes in CO_2 emissions, are denoted by subscript l, for relatively low CO_2 concentrations, *e.g.* HGO_l, and subscript h, for relatively high CO_2 concentrations, *e.g.* HGO_h. Fits shown in this figure are reproduced from data presented in Santos *et al.*[40]

analysis is advantageous in high spectral and spatial resolutions, and can be used to distinguish the mixing states of different functional groups, especially complicated carbon functional groups.[48] Samples for off-line STXM and NEXAFS analysis were collected on standard transmission electron microscopy (TEM) copper mesh grids (Ted Pella Inc.) using the Zurich electron microscope impactor (ZEMI). ZEMI is a custom built rotating drum impactor, developed at ETH Zürich in Switzerland. ZEMI holds a total of 24 TEM grids. During sampling, the sample stream containing the exhaust particles was directed onto the TEM grids. While exhaust particles impact and are trapped on the grids, gas molecules are aspirated. A detailed description of ZEMI is provided in Mahrt *et al.*[49] ZEMI sampled from the dilution unit as shown in Fig. 1. The sampling time within each individual case and grid was varied between 5 and 30 minutes.

Collected exhaust particle samples were inspected and analyzed at the BL4U beamline at the UVSOR Synchrotron Facility in Okazaki, Japan and at the SoftiMAX beamline at MAX IV laboratory in Lund, Sweden. With STXM/NEXAFS it is possible to resolve bonding and oxidation state information of sampled particles. Samples are subjected to soft X-rays that can be absorbed by core electrons. This absorption is influenced by several parameters, such as photon energy, elemental composition, sample thickness and density. When the photon energy approaches the ionization energy threshold, the photons excite corresponding core electrons and absorption occurs. This specific increase in absorption close to the ionization threshold is referred to as an absorption edge. For carbon, sharp peaks in NEXAFS spectra arise from electronic resonance transitions of different functional groups and involve both $1s \rightarrow \pi^*$ and/or $1s \rightarrow \sigma^*$ transitions. The NEXAFS peak positions and the relative intensities are used to determine functional groups and relative abundance(s) of the various functional groups that are present.[48] STXM/NEXAFS measurements were performed at the carbon K-edge (280–300 eV), nitrogen K-edge (393–425 eV), oxygen K-edge (525–550 eV) and sodium K-edge (1068–1095 eV) as well as L-edges for sulfur (159–196 eV), chlorine (190–210 eV) and calcium (343–357 eV).

Data analysis, including image alignments, selection of background regions and conversion of transmitted flux data was performed using AXIS 2000.[50]

3 Results and discussion

3.1 Particle size distributions and number emission factors (EF_{PN})

Particle emissions from combustion of the three fuel types as well as HGO with the WS using fresh- and seawater are shown in Fig. 2 in the form of (bimodal) lognormal size distributions. During the experiments performed by Santos *et al.*[40] sporadic variations in combustion conditions, presumably caused by fluctuations in the engine cooling system, were observed to also affect exhaust emissions. Combustion temperature has a significant effect on PM and soot formation within the cylinder. For diffusion flames, for example, the amount of soot formed increases monotonically with increasing combustion temperature.[51] As a result, sampling periods were further subcategorized using the subscripts h and l, referring to relatively low (l) or high (h) CO_2 concentrations measured in the raw exhaust during respective sampling periods. Variations of the same magnitude were not observed during CCN measurements.

Exhaust particles from combustion of HGO, MGO and HVO exhibit unimodal PSDs dominated by particle sizes in the ultrafine mode (d_{mo} < 100 nm) with CMDs between 45 nm and 53 nm (Fig. 2a). In both fresh- (FWS) and seawater (SWS) scrubbing scenarios the PSDs become bimodal (Fig. 2b), with a mode around 20 nm and a mode centered between 58 and 70 nm. Particles within the 20 nm mode are assumed to be formed *via* secondary pathways, originating from sulfuric acid droplets and other material condensing within the WS. Formation of these particles is favored by the strong reduction in exhaust gas temperature from ≈235 °C to ≈41 °C, relatively large amounts of gaseous SO_2 (>100 ppm) in the exhaust, possible oxidation of SO_2 to SO_3, as well as the generally high humidity caused by the water spraying within the WS. The aforementioned variability in combustion conditions becomes apparent when comparing FWS_h to the other wet scrubber cases, as seen from the distinct differences in peak ratios. In this case, the highest CO_2 concentrations of all cases were measured, suggesting that this sampling period was heavily affected by insufficient engine cooling which resulted in an altered emission profile.[40]

Calculated particle number emission factors (EF_{PN}) per kg of fuel consumed are presented in Fig. 3 and are also compared to other studies. Studies included in the comparison include measurements of both PM and CCN from large marine vessels or test-rig engines. In general, EF_{PN} vary from ≈5.6×10^{14} # kg^{-1} (HVO) to ≈1.1×10^{15} # kg^{-1} (SWS_l) and in most cases are about one order of magnitude smaller than other studies, including ships operating on both, low and high FSC fuels.[5,15–19] It is important to highlight that all of these studies are based on measurements of particulate emitted from generally, large marine vessels usually using much larger engines than the Volvo Penta engine used in this study. Moreover, in some of the studies[15,16] marine engines were operated on HFO which can vary substantially from distillate fuels with regard to its physicochemical properties, such as having significantly different viscosities and chemical compositions. Anderson *et al.*[7] studied particulate emissions from the same engine used in this study, at comparable engine loads, using two Swedish environmental class distillate fuels (MK1 and MK3), marine diesel oil and HFO. The EF_{PN} for MK1, MK3 and HFO from that study have been included in Fig. 3. Results obtained for MK1 and MK3 were in line with the results obtained in this study, at engine loads of 35% and 25%, where EF_{PN} varied between 2.3–2.9 × 10^{14} # kg^{-1} and 5.1–5.4 × 10^{14} # kg^{-1} respectively. Contrastingly, EF_{PN} were significantly increased when combusting HFO. At 25% engine load, for example, EF_{PN} reached 6 × 10^{17} # kg^{-1},[7] demonstrating how PM emissions can be strongly affected by fuel quality and combustion conditions.

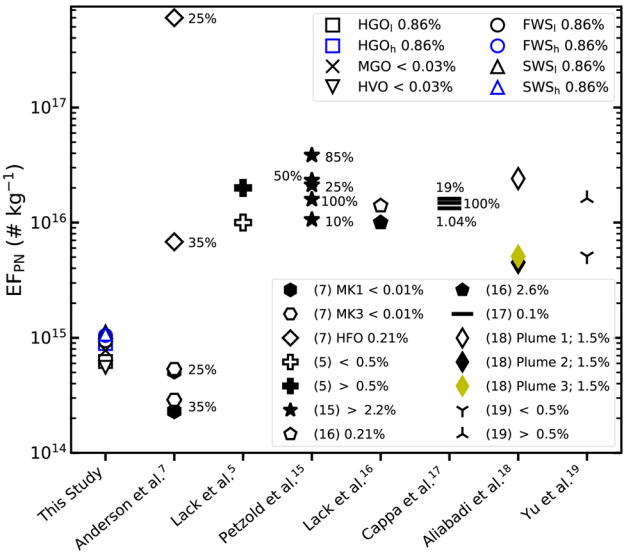

Fig. 3 Particle number emission factors (EF_{PN}) derived from integrated lognormal distributions (Fig. 2 and Santos *et al.*;[40] replotted in Fig. S2†). The values are compared to other studies. Anderson *et al.*[7] measured EF_{PN} for two low FSC distillate fuels (MK1 and MK3) and HFO (FSC = 0.12%) using the same engine and similar load conditions as in this study. Data provided by Lack *et al.*[5] is based on plume intercepts of ships categorized into high FSC (>0.5%) and low FSC (<0.5%) fuel consumption. Petzold *et al.*[15] results are based on experiments with a large 4-stroke test-rig engine at different engine loads using HFO with an FSC between ≈2.2 and ≈2.3%. Lack *et al.*[16] intercepted plumes of a large container vessel using HFO with a FSC = 2.6% and MGO with a FSC = 0.21%. Cappa *et al.*[17] derived EF_{PN} from plume intercepts of an older marine vessel operating on 0.1% FSC fuel at different engine loads. Results from Aliabadi *et al.*[18] are based on plume intercepts of a marine vessel operating on 1.5% FSC fuel at relatively low loads. Yu *et al.*[19] measured EF_{PN} in plumes of ships using either low (<0.5%) or high FSC (>0.5%) fuels. Percentages in the figure either indicate FSC (legend) or engine load (next to data points).

3.2 Critical supersaturations (SS_c) and κ values

CCN activities and particle hygroscopicities are presented in the form of averaged case and size dependent SS_c and κ values in Fig. 4. As shown in Fig. 2 variations in combustion conditions affect PM emissions. Moreover, changes in combustion conditions, such as differences in combustion temperature, have significant effects on PM and gaseous emissions from engines.[51] The amount of condensed matter on exhaust particles and degree of oxidation are strongly linked to combustion parameters and ultimately, also affect the water uptake abilities of emitted particulate. However, the observed variability in absolute emission characteristics (PM, CO_2, *etc.*) was not observed to propagate to CCN activity and thus averaged cases are presented that represent the full range of combustion conditions.

In all cases shown in Fig. 4a a decrease in required SS_c with increasing particle size is observed which has previously been reported for engine combustion particles.[4,22,52] In general, the pathways to achieve regulatory FSC compliance, *i.e.* switching from high to low FSC marine fuels or using high FSC fuels with exhaust gas wet scrubbing, yield opposing effects regarding the CCN activation of fresh exhaust particles. Switching to low FSC fuels resulted in significantly increased SS_c required to form cloud droplets. Moreover, when comparing MGO and HVO, results indicate that a reduction in organic PM precursors further reduces CCN activity. Combustion of HVO resulted in emissions of highly hydrophobic exhaust particles, which did not show any sign of CCN activity even at the largest ΔT setting (18 °C),

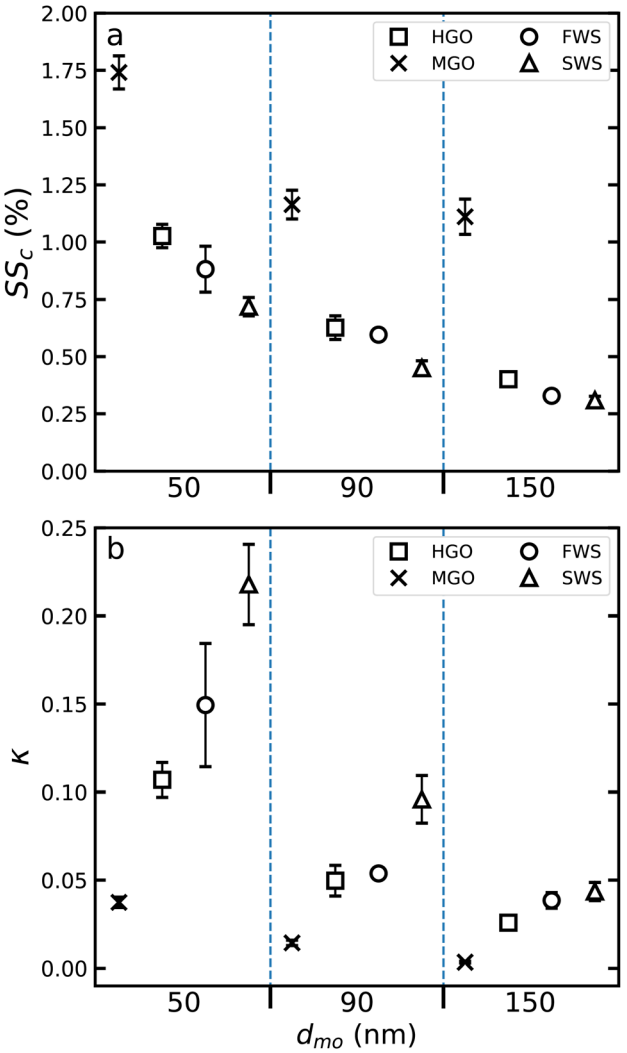

Fig. 4 (a) Critical supersaturations SS_c and (b) κ values of fresh exhaust particles obtained for mobility diameters of 50 nm, 90 nm and 150 nm. HGO and MGO designate exhaust particles produced from the combustion of the respective fuels, whereas FWS and SWS indicate HGO combustion in conjunction with wet scrubbing using either sea- (SWS) or freshwater (FWS). The CCN activity was below the detection limit for HVO particles, and therefore HVO related data points are not present in the figure. Data points are calculated mean values with whiskers indicating measurement uncertainties given by ± 1 standard deviation.

corresponding to a maximum achievable supersaturation of 2.4%. While HVO data are excluded in Fig. 4, we can estimate for HVO a SS_c > 2.5%. For MGO measured SS_c values were larger compared to HGO. Activation of MGO particles required SS_c > 1% for all particle sizes. Such high SS_c values are in line with other studies investigating droplet formation from freshly-emitted, low sulfur content diesel exhaust particles.[22,52,53]

Both WS cases, on the other hand, facilitated more efficient droplet formation as seen from the reduced SS_c values compared to HGO (Fig. 4a). Wet scrubbing can also have secondary effects on exhaust particles, such as affecting the chemical composition, mixing state and morphology[39] as well as the effective density,[40] and consequently the amount of condensed material, which can impact the water uptake of exhaust particles. Lieke *et al.*[39] describe the effects of wet scrubbing on particulate matter as a substantially accelerated atmospheric aging process. Therein, the authors observe that scrubbed exhaust particles collapsed and had more dense, ball-like structures as well as larger fractions of water soluble compounds compared to unscrubbed exhaust particles.[39] Scrubbing with seawater (SWS) decreased the droplet formation threshold even further compared to freshwater scrubbing (FWS). A larger fraction of more hydrophilic salt condensates, for example, could explain this observation, which is supported by earlier observations where seawater scrubbing led to increased effective densities compared to freshwater usage.[40]

Observed SS_c trends are also reflected in the average calculated κ values, which vary between 0.04 (MGO) and 0.22 (SWS) for 50 nm particles and 0 (MGO) and 0.03 (SWS) for 150 nm particles (Fig. 4b). These κ values agree well with literature results for the hygroscopicity of engine combustion particles.[22] Assuming that SS_c for 50 nm, 90 nm and 150 nm HVO particles is equal to 2.5%, one can derive conservative κ estimates of 0.018, 0.003 and 0.001 respectively. It is important to note, that actual SS_c values for HVO particles might be significantly larger than 2.5%, implying that actual κ values may be even lower.

3.3 Chemical characterization and mixing state of emitted soot particles

Fig. 5a shows the carbon K-edge NEXAFS spectra of collected soot particles for four of the five cases. No soot particles were collected for the HVO case, though the same sampling procedures were applied. Sulfur L-edge spectra are displayed in a separate panel (Fig. 5b). A common feature in all carbon spectra is the peak at ≈285.4 eV, which is the characteristic transition of sp^2 hybridized carbon (doubly bonded carbon)[54] that is abundant in soot or elemental carbon.[55] At ≈287.4 eV, a component corresponding to carbonyl (C=O)[56] appears in some spectra, SWS_1, FWS_1 and MGO_1 and MGO_2 samples. In some cases an extended distribution around ≈288.6 eV appears, which refers to carboxyl groups (COOH).[48,56] The relative heights of these peaks vary between cases, which implies a heterogeneity of organic(s) mixing with soot particles. Moreover, a broad component around 292 eV is indicative of the σ* transition of C–C bonds in all cases. Together with the double bond at 285.4 eV, these carbon–carbon bonds are commonly found in soot and graphite.[57]

In Fig. 5b, sulfate can be identified by its fingerprint peaks at ≈173.5 eV and ≈182 eV in the cases with sulfur-containing fuel,[58,59] *i.e.* HGO_1, SWS_1 and FWS_1. Similar to the heterogeneity observed for organics, sulfate is not necessarily present in all particles from HGO and WS related particles. No obvious correlations between the COOH/C=O groups and sulfate are observed. For the sulfur-free MGO, no sulfates were detected, which confirms that the sulfur source in the other cases is the fuel itself or traces in the seawater or -salt, which cannot be excluded for both SWS cases. The presence of sulfate in SWS and FWS cases indicates that the scrubbing process does not remove sulfur that is already in the particulate phase.

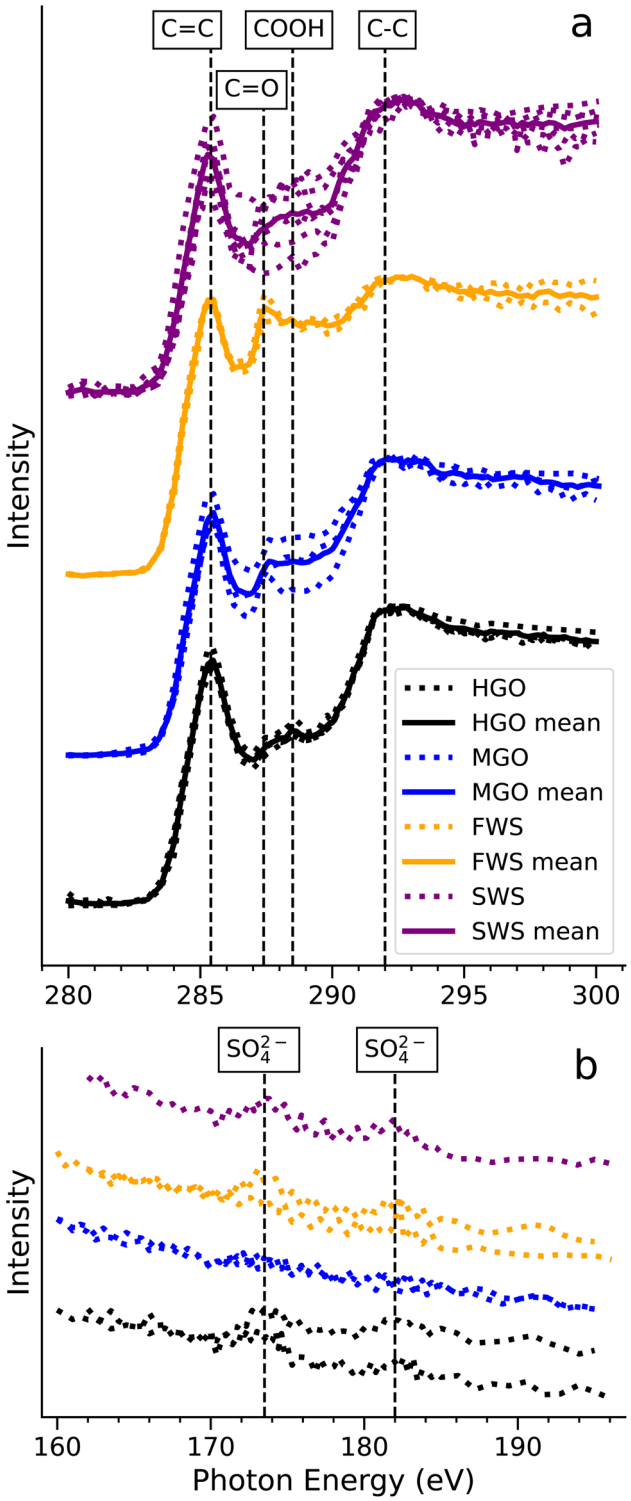

Fig. 5 Near edge X-ray absorption fine structure (NEXAFS) spectra of HGO, MGO, FWS and SWS particles, (a) measured at the carbon K-edge and (b) at the sulfur L-edge. HGO and MGO designate exhaust particles produced from the combustion of the respective fuels, whereas FWS and SWS indicate HGO combustion in conjunction with wet scrubbing using either sea- (SWS) or freshwater (FWS). Spectra haven been grouped for each individual case and shifted vertically for better differentiation. Dotted lines represent spectra of individual particles and solid lines are averaged spectra.

In order to investigate, whether compounds associated with salts in the seawater partition into the particle phase, several SWS particles were inspected for sodium (Fig. 6) and chlorine (Fig. S4†). While no significant signals of chlorine were detected, other inspected particles showed that seawater scrubbing affected their mixing states, both internally and externally. Fig. 6 shows an image of SWS particles and carbon, sodium and oxygen NEXAFS spectra for corresponding areas marked on the particles. Results show both externally mixed soot and inorganic salt particles as well as internally mixed soot particles with salt fractions on the particle surfaces. We assume that salt fractions on soot surfaces are formed during or after the scrubbing process *via* condensation, coagulation, collisional transfer between externally mixed particles, or perhaps contact efflorescence whereby refractory soot particles act as the seeds to stimulate salt efflorescence as the relative humidity decreases after scrubbing.[60] Moreover, in the case of SWS, an inhomogeneous agglomerate consisting of an inorganic salt particle, a column-shaped mineral particle as well as a soot particle was found (Fig. S7†). Similarly mixed particles could not be observed for HGO, MGO and FWS which indicates that the origin of observed salt and mineral particles is likely the seawater itself.

Taken as a whole, the results suggest that the comparatively high CCN activities for FWS, SWS as well as HGO result primarily from larger fractions of hygroscopic sulfate components in the particulate phase. Furthermore, NEXAFS spectra reveal salt fractions in the particulate phase of SWS particles which is a possible explanation for the observed increase in CCN activity compared to the other cases. While larger externally mixed (sea)salt particles could be observed, no qualitative differences in CCN activation spectra between SWS and FWS could be observed, which indicates that for the investigated mobility diameters pure salt particles do not comprise a significant amount of CCN emissions. As for the MGO samples, we found an extraordinarily low level of sulfate as well as low measured CCN activities.

3.4 CCN emission factors

CCN emission factors (EF_{CCN}) as a function of SS are shown in Fig. 7 for the exhaust with measured CCN activity. MGO yields the smallest EF_{CCN} which is caused by the reduced hygroscopicity (Fig. 4) given the differences in PSDs between MGO and HGO_l (Fig. 2). When using average values of both HGO cases as a baseline, at SS values of 0.3% and 0.7% EF_{CCN} were reduced by $\approx$91.1% and $\approx$91.5% respectively. On the other hand, a clear distinction in EF_{CCN} between HGO and WS cases is not immediately apparent, suggesting that CCN emissions are limited by both hygroscopicity and the size of emitted exhaust particles. Within Fig. 7, the inset panel shows the SS range from 0 to 0.3% in detail, which is a good approximation of the supersaturation range for Arctic mixed-phase clouds. In this SS range EF_{CCN} seem to be more affected by particle size than by increased hygroscopicity from wet scrubbing, as seen from the increased HGO_h CCN emissions compared to most wet scrubber cases. Nevertheless, results also show that seawater scrubbing leads to increased EF_{CCN} emissions compared to freshwater scrubbing (compare, for example, SWS_h and FWS_l which exhibit very

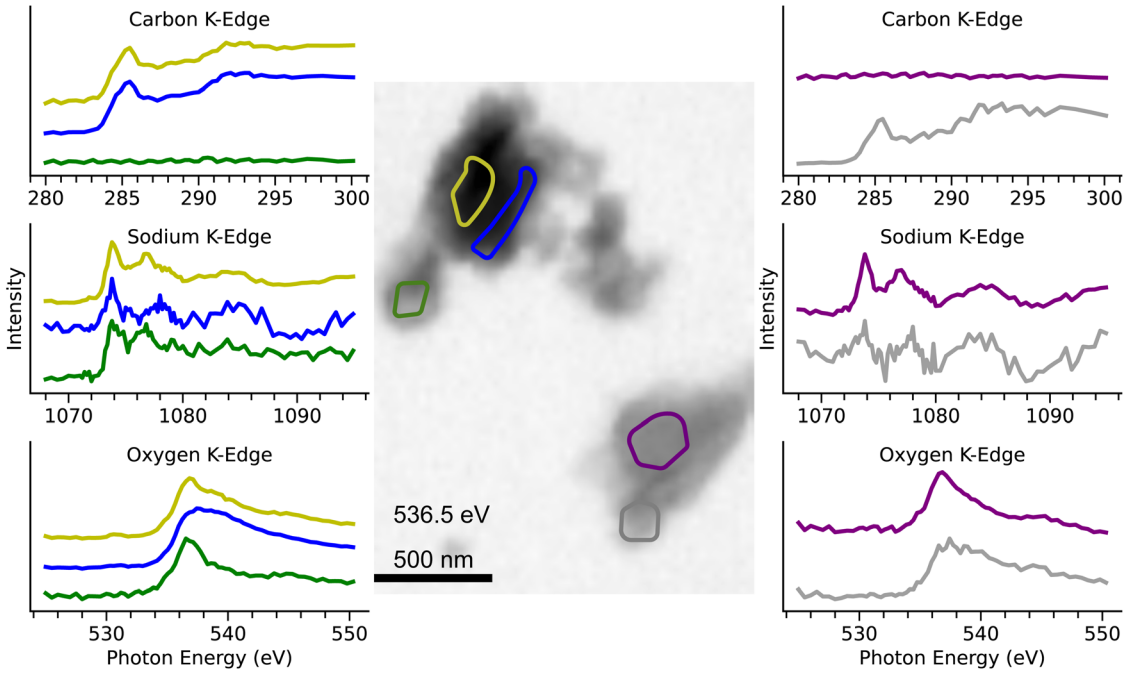

Fig. 6 STXM image of SWS particles (center panel) and NEXAFS K-edges of carbon, sodium and oxygen. Individual spectra correspond to the regions on the particles marked with the respective colors.

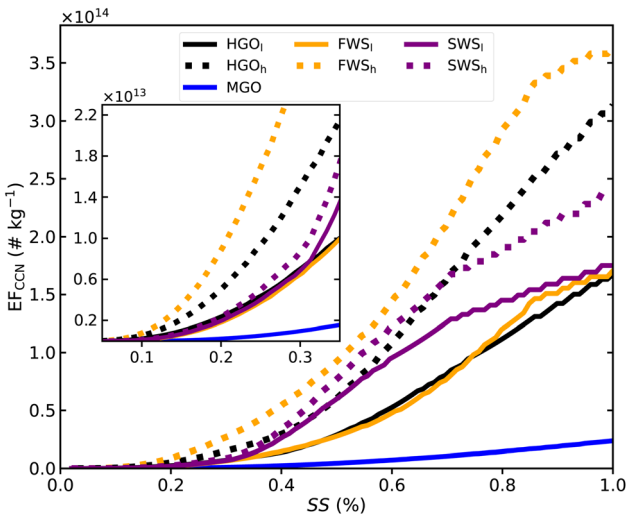

Fig. 7 CCN emission factors (EF_{CCN}) normalized relative to fuel consumption as function of supersaturation (SS) for each case where CCN activity was observed. EF_{CCN} were calculated using (bimodal) lognormal distributions representing particulate emissions for each case (Fig. 2) and CCN activity derived from inter- and extrapolated κ values (Fig. 4b). Observed differences in combustion conditions for HGO, FWS and SWS are denoted by subscript l for relatively low CO_2 concentrations, *e.g.* HGO_l, and subscript h for relatively high CO_2 concentrations, *e.g.* HGO_h.

similar PSDs). This can be attributed to the higher salinity and the generally greater heterogeneity of seawater in terms of chemical composition compared to freshwater.

Random errors for EF_{CCN} were estimated using measured variability in PN concentrations, κ for 50, 90 and 150 nm, as well as estimated relative uncertainties of 10% for the fuel consumption and exhaust flow rate(s). We find that depending on the κ uncertainty for the respective sizes and cases, EF_{CCN} display relative uncertainties between 18% and 36%. Moreover, our assumption of constant κ values for particles larger than 150 nm introduces further uncertainties in EF_{CCN} estimates, especially for SS values below 0.3%, *i.e.* EF_{CCN} in this range are, depending on the case, overestimated to various degrees. Given the relatively small amount of emitted particles larger than 150 nm, we expect this uncertainty to have a limited effect on our main observations.

In Fig. 8 calculated CCN emission factors are compared to other available data for different ship, engine and fuel types as well as different SS. Comparisons are made at 0.3%, 0.44%, 0.6% and 0.7% of SS. Relative reductions in EF_{CCN} caused by a switch to low FSC fuels are also observed in other studies.[5,15,19] Lower FSC has been shown to lower the amounts of particulate-phase sulfuric acid coating[4] and sulfates,[19] reducing the water-soluble fraction of exhaust particles and hence, their CCN activity. Calculated EF_{CCN} are generally much smaller than those derived from plume measurements of ships using high FSC fuels, specifically HFO.[5,16] However, results for the HGO and WS cases agree well with those of ships using low FSC fuels. As previously discussed and shown in Fig. 3, we assume that these discrepancies have different origins. First, comparing emissions from different ships or diesel engines can be difficult. The Volvo Penta D3 engine used in this study can vary quite substantially from those used on-board ships in the cited literature. Large marine vessels, such as container ships, are often equipped with large 2-stroke diesel engines, which affects particulate emissions. Secondly, the engine operating mode,

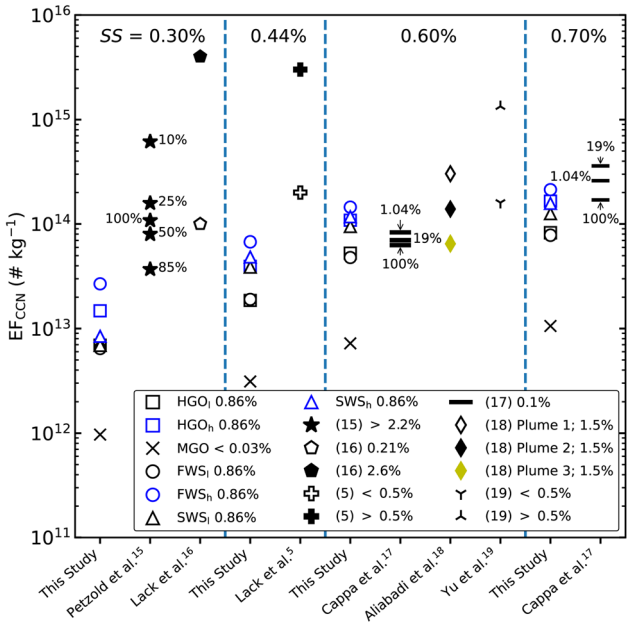

Fig. 8 Calculated EF_{CCN} are compared to literature values from ships or ship engines at supersaturations (SS) of 0.3%, 0.44%, 0.6% and 0.7%. Percentages in the figure either indicate SS (top row), FSC (legend) or engine load (next to data points). Data provided by Lack *et al.*[5] are based on plume intercepts of ships categorized into high FSC (>0.5%) and low FSC (<0.5%) fuel consumption. Petzold *et al.*[15] results are based on experiments with a large 4-stroke test-rig engine at different engine loads (denoted by the percentages next to the data points) using HFO with an FSC between ≈2.2 and ≈2.3%. Lack *et al.*[16] intercepted plumes of a large container vessel using HFO with a FSC = 2.6% and MGO with a FSC = 0.21%. Cappa *et al.*[17] derived EF_{CCN} from plume intercepts of an older vessel operating on 0.1% FSC fuel at different engine loads (indicated by the percentages). Results from Aliabadi *et al.*[18] are based on plume intercepts of a marine vessel operating on 1.5% FSC fuel at relatively low loads. Yu *et al.*[19] measured EF_{CCN} in plumes of ships using either low (<0.5%) or high FSC (>0.5%) fuels.

e.g. differences in engine load, as well as larger consumption of lubricating oil have effects on PM emissions. These differences usually affect the size distributions, number concentrations and chemical compositions of exhaust particles. As shown in Fig. 7, differences in EF_{CCN} for HGO and WS are mostly constrained by the measured particle size distributions rather than differences in hygroscopicities. Lack *et al.*,[16] for example, observed a substantial shift towards smaller sizes in emitted particles when the investigated container ship switched from HFO to low FSC MGO and concluded that the measured reduction in EF_{CCN} was primarily caused by changes to the PSD rather than a decrease in hygroscopicity. Similarly, Yu *et al.*[19] observed a larger mode in PSDs (70–80 nm) measured in plumes of ships operating on the open sea (high FSC) compared to plume measurements conducted within a SECA (30–50 nm) and concluded that changes in EF_{CCN} were induced both by changes in PSDs as well as chemical composition of exhaust particles.

Activated fractions (AF), *i.e.* the fraction of particles activated into droplets at a given SS expressed in [%], ranged from 0.1% (MGO) to 2.6% (FWS_h) at SS of 0.3% and increased to 1.4% (MGO) and 20.3% (FWS_h) at SS of 0.7%. AF as low as those calculated for MGO, even at relatively high SS, have previously been reported by Cappa *et al.*[17] who measured CCN emissions of a ship operating on 0.1% FSC fuel. In contrast, other studies[5,16] report activation ratios between 40% and 42% for high FSC fuels at SS of 0.3% and 0.44% respectively, although AF are, in general, sensitive to the experimental setup and thus, difficult to compare between different studies.

4 Atmospheric implications

Results presented in this study show that pathways to international fuel sulfur content regulatory compliance may have opposing effects on CCN activity of fresh exhaust particles emitted by marine diesel engines. These observations may have implications for atmospheric processes, clouds and regional climate. One region of interest where shipping activity is projected to increase in the future and where associated airborne emissions might affect regional climate due to relatively low background concentrations of various pollutants is the Arctic.[27,61–63] In particular, Arctic low-level mixed-phase clouds, which can sustain themselves over extended periods of time compared to those of lower latitudes, are a key aspect to understanding climatological responses.[64] Gilgen *et al.*[27] highlight that the indirect aerosol-cloud net-effect of increased ship emissions is cooling but is insufficient to counteract other changes induced by the enhanced warming, such as a general decrease in surface albedo, which has a net warming effect. It is important to note, that Gilgen *et al.*[27] use emission inventories from Peters *et al.*[61] which include significant reductions in emission factors of SO_2 and BC but not potential secondary effects of different fuels and abatement technologies as presented in this study. Conversely, Stephenson *et al.*[63] found that future trans-Arctic shipping can potentially suppress Arctic warming by 1 °C by 2099, using different emission inventories.

Once emitted into the atmosphere, exhaust particles will undergo processes that affect their physicochemical properties. For exhaust particles transported from lower, more anthropogenically affected latitudes, aging processes, *i.e.* surface and photochemistry, are key aspects in increasing the hygroscopicity of aerosol particles.[21–23,65] Similarly, we observe the particle population emitted from seawater scrubbing to be significantly altered with regards to its general mixing state. Interspersed with salt particles we detected salt condensates as well as sulphates on the surface of scrubbed soot particles. These particles and their hygroscopic fractions can promote water vapor adsorption and potential unique interfacial chemistry even at low RH.[66] In this study we estimate CCN emissions based on CCN activity of combustion particles but especially in the case of wet scrubbing, emission of inorganic salt particles can be an important source of CCN.

Bulatovic *et al.*[67] have shown that SS in Arctic mixed-phase clouds can be sufficiently large to activate Aitken mode particles (d_{mo} ≈ 25–80 nm) into cloud droplets. They also found that particles did not have to be very hygroscopic and that κ values of ≈0.1 were sufficient for CCN activation that extends cloud lifetime.[67] This implies that κ values for 50 nm FWS (0.15) and SWS (0.22) particles are sufficiently large to become CCN active

in this environment. The derived κ value for HGO at 50 nm (0.11) is very close to the threshold, whereas fresh 50 nm MGO particles (0.04) would likely not act as CCN. It is important to note, that the activation process depends on several things, including the concentration of larger accumulation mode particles as these can serve as scavengers for water vapor and inhibit activation of smaller particles. Low concentrations of larger accumulation mode particles are often encountered in the high Arctic where an increase in CCN concentrations can have large effects on the aerosol indirect effect.[68] The potential for increased CCN activity, due to WS exhaust particles, to lead to net cooling should be further investigated with aerosol, cloud, climate modeling.

The discussed IMO regulations have a large impact on the shipping sector where companies and ship operators have to decide whether to use low FSC fuels or wet scrubbing in order to meet compliance standards. Given the opposing effects we observe for compliance measures on the CCN activity of fresh exhaust particles and what this implies, for example, for Arctic mixed-phase clouds and regional climate, it is important to further investigate how the shipping sector will evolve in the coming decades.

5 Conclusions

Here, we investigated how international maritime fuel sulfur content restrictions may impact the CCN activity of fresh ship exhaust particles. One non-compliant, high FSC fuel was used, HGO, as well as two compliant, low FSC fuels, MGO and HVO. In addition, we investigated how wet scrubbing affected the CCN activity of HGO exhaust particles using both sea- and freshwater. CCN measurements were performed on 50, 90 and 150 nm (d_{mob}) exhaust particles using a DMT CCN counter in SFCA operation mode.[45] Chemical compositions of particulate were studied using STXM and NEXAFS measurements.

Our results demonstrate that the investigated compliance measures can have opposing effects on the water uptake ability of fresh exhaust particles. Combustion of the low FSC fuels, showed significant reductions in CCN activity compared to the high FSC fuel (HGO). HVO particles proved to be highly hydrophobic, rendering it impossible to calculate EF_{CCN}. Similarly, MGO particles required higher SS to induce droplet activation. Consequently, EF_{CCN} were significantly reduced for MGO compared to HGO. At an atmospherically relevant supersaturation of 0.3%, EF_{CCN} were reduced by $\approx$91%. These observations agree with other studies investigating the effect of FSC reduction on CCN emissions from ships.[5,16,19]

Wet scrubbing, on the other hand, reduced the SS threshold for CCN activation for HGO. These observations support earlier findings showing that wet scrubbing has secondary effects on ship exhaust particles, *e.g.* by increasing the amount of condensable material as well as changing the structure and morphology of the particles.[39,40] The results are supported by NEXAFS spectra that show traces of sulfates and salt condensates on soot particles. When operating the WS with seawater, particles displayed greater CCN activity. We assume that increased CCN activity was caused by larger salt fractions. Nevertheless, observed increases in CCN activity for WS cases did not yield significantly larger EF_{CCN}. EF_{CCN} were limited by particle number concentrations and size distributions. Measured EF_{CCN} for ships using high FSC fuels and reported for ocean-going ships often yield values one order of magnitude greater than the largest EF_{CCN} calculated in this study.[5,15,16,19] However, it is important to highlight, that compared to our engine, large marine vessels often emit both, physically larger as well as larger amounts of exhaust particles. Moreover, we cannot exclude whether the temperature controlled dilution system in our experiments reduces CCN emissions compared to real-world dilution of exhaust gas in the atmosphere.

Considering the general lack of studies and reported discrepancies with regard to the effects of wet scrubbing on particulate matter emissions from ships, it is important to consider potential unforeseen climatological effects. Future ship exhaust studies should not only focus on particle removal efficiencies of on-board wet scrubbing but also investigate secondary effects that might have atmospheric relevance.

Author contributions

LS wrote the manuscript with contributions from EST, XK, KS, TBK, JN and TO. LS, KS and EST designed the majority of the experiments. LS and KS conducted the engine experiments and operated gas instrumentation and the dilution system. LS operated all aerosol instrumentation, analyzed gas, SMPS and CCN data and created all figures. LS, TBK and EST interpreted the CCN data. LS and XK collected off-line samples using ZEMI, analyzed STXM/NEXAFS data and wrote related sections. LS and XK conducted STXM/NEXAFS measurements at MAX IV, Sweden. JN and TO conducted STXM/NEXAFS measurements at UVSOR, Japan. All authors contributed to the interpretation of the results. EST supervised the project.

Conflicts of interest

There are no conflicts to declare.

Acknowledgements

This research was funded by the Swedish Research Councils FORMAS (2017-00564) and VR (2013-05153, 2020-03497 & 2021-04042). A part of this work was performed at the BL4U of UVSOR Synchrotron Facility, Institute for Molecular Science (IMS program 20-750). We acknowledge MAX IV Laboratory for time on Beamline SoftiMAX under Proposal 20200683. Research conducted at MAX IV, a Swedish national user facility, is supported by the Swedish Research council under contract 2018-07152, the Swedish Governmental Agency for Innovation Systems under contract 2018-04969, and Formas under contract 2019-02496. EST and LS thank the Swedish Strategic Research Area MERGE for support. We would like to thank Zamin A. Kanji from ETH and Fabian Mahrt from PSI for use of and assistance with ZEMI and helpful discussions. X. K. acknowledges the support from the Swedish Foundation for International Cooperation in Research and Higher Education (CH2019-8361).

Notes and references

1 N. Kuittinen, J.-P. Jalkanen, J. Alanen, L. Ntziachristos, H. Hannuniemi, L. Johansson, P. Karjalainen, E. Saukko, M. Isotalo, P. Aakko-Saksa, K. Lehtoranta, J. Keskinen, P. Simonen, S. Saarikoski, E. Asmi, T. Laurila, R. Hillamo, F. Mylläri, H. Lihavainen, H. Timonen and T. Rönkkö, Shipping Remains a Globally Significant Source of Anthropogenic PN Emissions Even after 2020 Sulfur Regulation, *Environ. Sci. Technol.*, 2021, **55**, 129–138.

2 J. Moldanová, E. Fridell, H. Winnes, S. Holmin-Fridell, J. Boman, A. Jedynska, V. Tishkova, B. Demirdjian, S. Joulie, H. Bladt, N. P. Ivleva and R. Niessner, Physical and chemical characterisation of PM emissions from two ships operating in European Emission Control Areas, *Atmos. Meas. Tech.*, 2013, **6**, 3577–3596.

3 O. Sippula, B. Stengel, M. Sklorz, T. Streibel, R. Rabe, J. Orasche, J. Lintelmann, B. Michalke, G. Abbaszade, C. Radischat, T. Gröger, J. Schnelle-Kreis, H. Harndorf and R. Zimmermann, Particle Emissions from a Marine Engine: Chemical Composition and Aromatic Emission Profiles under Various Operating Conditions, *Environ. Sci. Technol.*, 2014, **48**, 11721–11729.

4 A. Petzold, M. Gysel, X. Vancassel, R. Hitzenberger, H. Puxbaum, S. Vrochticky, E. Weingartner, U. Baltensperger and P. Mirabel, On the effects of organic matter and sulphur-containing compounds on the CCN activation of combustion particles, *Atmos. Chem. Phys.*, 2005, **5**, 3187–3203.

5 D. A. Lack, J. J. Corbett, T. Onasch, B. Lerner, P. Massoli, P. K. Quinn, T. S. Bates, D. S. Covert, D. Coffman, B. Sierau, S. Herndon, J. Allan, T. Baynard, E. Lovejoy, A. R. Ravishankara and E. Williams, Particulate emissions from commercial shipping: Chemical, physical, and optical properties, *J. Geophys. Res.: Atmos.*, 2009, **114**, 1–16.

6 M. Anderson, K. Salo and E. Fridell, Particle- and Gaseous Emissions from an LNG Powered Ship, *Environ. Sci. Technol.*, 2015, **49**, 12568–12575.

7 M. Anderson, K. Salo, Å. M. Hallquist and E. Fridell, Characterization of particles from a marine engine operating at low loads, *Atmos. Environ.*, 2015, **101**, 65–71.

8 J. Alanen, M. Isotalo, N. Kuittinen, P. Simonen, S. Martikainen, H. Kuuluvainen, M. Honkanen, K. Lehtoranta, S. Nyyssönen, H. Vesala, H. Timonen, M. Aurela, J. Keskinen and T. Rönkkö, Physical Characteristics of Particle Emissions from a Medium Speed Ship Engine Fueled with Natural Gas and Low-Sulfur Liquid Fuels, *Environ. Sci. Technol.*, 2020, **54**, 5376–5384.

9 P. Eichler, M. Müller, C. Rohmann, B. Stengel, J. Orasche, R. Zimmermann and A. Wisthaler, Lubricating Oil as a Major Constituent of Ship Exhaust Particles, *Environ. Sci. Technol. Lett.*, 2017, **4**, 54–58.

10 E. Fridell, E. Steen and K. Peterson, Primary particles in ship emissions, *Atmos. Environ.*, 2008, **42**, 1160–1168.

11 D. E. Schraufnagel, The health effects of ultrafine particles, *Exp. Mol. Med.*, 2020, **52**, 311–317.

12 J. J. Corbett, J. J. Winebrake, E. H. Green, P. Kasibhatla, V. Eyring and A. Lauer, Mortality from Ship Emissions: A Global Assessment, *Environ. Sci. Technol.*, 2007, **41**, 8512–8518.

13 J. J. Winebrake, J. J. Corbett, E. H. Green, A. Lauer and V. Eyring, Mitigating the health impacts of pollution from oceangoing shipping: An assessment of low-sulfur fuel mandates, *Environ. Sci. Technol.*, 2009, **43**, 4776–4782.

14 N. Bellouin, J. Quaas, E. Gryspeerdt, S. Kinne, P. Stier, D. Watson-Parris, O. Boucher, K. S. Carslaw, M. Christensen, A. L. Daniau, J. L. Dufresne, G. Feingold, S. Fiedler, P. Forster, A. Gettelman, J. M. Haywood, U. Lohmann, F. Malavelle, T. Mauritsen, D. T. McCoy, G. Myhre, J. Mülmenstädt, D. Neubauer, A. Possner, M. Rugenstein, Y. Sato, M. Schulz, S. E. Schwartz, O. Sourdeval, T. Storelvmo, V. Toll, D. Winker and B. Stevens, Bounding Global Aerosol Radiative Forcing of Climate Change, *Rev. Geophys.*, 2020, **58**, 1–45.

15 A. Petzold, E. Weingartner, J. Hasselbach, P. Lauer, C. Kurok and F. Fleischer, Physical properties, chemical composition, and cloud forming potential of particulate emissions from a marine diesel engine at various load conditions, *Environ. Sci. Technol.*, 2010, **44**, 3800–3805.

16 D. A. Lack, C. D. Cappa, J. Langridge, R. Bahreini, G. Buffaloe, C. Brock, K. Cerully, D. Coffman, K. Hayden, J. Holloway, B. Lerner, P. Massoli, S.-M. Li, R. McLaren, A. M. Middlebrook, R. Moore, A. Nenes, I. Nuaaman, T. B. Onasch, J. Peischl, A. Perring, P. K. Quinn, T. Ryerson, J. P. Schwartz, R. Spackman, S. C. Wofsy, D. Worsnop, B. Xiang and E. Williams, Impact of Fuel Quality Regulation and Speed Reductions on Shipping Emissions: Implications for Climate and Air Quality, *Environ. Sci. Technol.*, 2011, **45**, 9052–9060.

17 C. D. Cappa, E. J. Williams, D. A. Lack, G. M. Buffaloe, D. Coffman, K. L. Hayden, S. C. Herndon, B. M. Lerner, S. M. Li, P. Massoli, R. McLaren, I. Nuaaman, T. B. Onasch and P. K. Quinn, A case study into the measurement of ship emissions from plume intercepts of the NOAA ship Miller Freeman, *Atmos. Chem. Phys.*, 2014, **14**, 1337–1352.

18 A. A. Aliabadi, J. L. Thomas, A. B. Herber, R. M. Staebler, W. R. Leaitch, H. Schulz, K. S. Law, L. Marelle, J. Burkart, M. D. Willis, H. Bozem, P. M. Hoor, F. Köllner, J. Schneider, M. Levasseur and J. P. Abbatt, Ship emissions measurement in the Arctic by plume intercepts of the Canadian Coast Guard icebreaker Amundsen from the Polar 6 aircraft platform, *Atmos. Chem. Phys.*, 2016, **16**, 7899–7916.

19 C. Yu, D. Pasternak, J. Lee, M. Yang, T. Bell, K. Bower, H. Wu, D. Liu, C. Reed, S. Bauguitte, S. Cliff, J. Trembath, H. Coe and J. D. Allan, Characterizing the Particle Composition and Cloud Condensation Nuclei from Shipping Emission in Western Europe, *Environ. Sci. Technol.*, 2020, **54**, 15604–15612.

20 T. C. Bond, S. J. Doherty, D. W. Fahey, P. M. Forster, T. Berntsen, B. J. Deangelo, M. G. Flanner, S. Ghan, B. Kärcher, D. Koch, S. Kinne, Y. Kondo, P. K. Quinn, M. C. Sarofim, M. G. Schultz, M. Schulz, C. Venkataraman,

H. Zhang, S. Zhang, N. Bellouin, S. K. Guttikunda, P. K. Hopke, M. Z. Jacobson, J. W. Kaiser, Z. Klimont, U. Lohmann, J. P. Schwarz, D. Shindell, T. Storelvmo, S. G. Warren and C. S. Zender, Bounding the role of black carbon in the climate system: A scientific assessment, *J. Geophys. Res.: Atmos.*, 2013, **118**, 5380–5552.

21 J. Pagels, A. F. Khalizov, P. H. McMurry and R. Y. Zhang, Processing of soot by controlled sulphuric acid and water condensation mass and mobility relationship, *Aerosol Sci. Technol.*, 2009, **43**, 629–640.

22 C. Wittbom, A. C. Eriksson, J. Rissler, J. E. Carlsson, P. Roldin, E. Z. Nordin, P. T. Nilsson, E. Swietlicki, J. H. Pagels and B. Svenningsson, Cloud droplet activity changes of soot aerosol upon smog chamber ageing, *Atmos. Chem. Phys.*, 2014, **14**, 9831–9854.

23 X. Pei, M. Hallquist, A. C. Eriksson, J. Pagels, N. M. Donahue, T. Mentel, B. Svenningsson, W. Brune and R. K. Pathak, Morphological transformation of soot: Investigation of microphysical processes during the condensation of sulfuric acid and limonene ozonolysis product vapors, *Atmos. Chem. Phys.*, 2018, **18**, 9845–9860.

24 M. W. Christensen, K. Suzuki, B. Zambri and G. L. Stephens, Ship track observations of a reduced shortwave aerosol indirect effect in mixed-phase clouds, *Geophys. Res. Lett.*, 2014, **41**, 6970–6977.

25 A. Possner, E. Zubler, U. Lohmann and C. Schär, The resolution dependence of cloud effects and ship-induced aerosol-cloud interactions in marine stratocumulus, *J. Geophys. Res.*, 2016, **121**, 4810–4829.

26 E. S. Thomson, D. Weber, H. G. Bingemer, J. Tuomi, M. Ebert and J. B. C. Pettersson, Intensification of ice nucleation observed in ocean ship emissions, *Sci. Rep.*, 2018, **8**, 1111.

27 A. Gilgen, W. T. K. Huang, L. Ickes, D. Neubauer and U. Lohmann, How important are future marine and shipping aerosol emissions in a warming Arctic summer and autumn?, *Atmos. Chem. Phys.*, 2018, **18**, 10521–10555.

28 M. S. Diamond, H. M. Director, R. Eastman, A. Possner and R. Wood, Substantial Cloud Brightening From Shipping in Subtropical Low Clouds, *AGU Adv*, 2020, **1**, 1–28.

29 F. Glassmeier, F. Hoffmann, J. S. Johnson, T. Yamaguchi, K. S. Carslaw and G. Feingold, Aerosol-cloud-climate cooling overestimated by ship-track data, *Science*, 2021, **371**, 485–489.

30 International Maritime Organisation, *Revised MARPOL Annex VI - Amendments to the Annex of the Protocol of 1997 to amend the International Convention for the Prevention of Pollution from Ships, 1973, as Modified by the Protocol of 1978 Relating Thereto (MEPC.176(58))*, 2008.

31 International Maritime Organisation, *2015 Guidelines for Exhaust Gas Cleaning Systems (MEPC.259(68))*, International maritime organization technical report, 2015.

32 K. Oikawa, C. Yongsiri, K. Takeda and T. Harimoto, Seawater flue gas desulfurization: Its technical implications and performance results, *Environ. Prog.*, 2003, **22**, 67–73.

33 A. Andreasen and S. Mayer, Use of seawater scrubbing for SO_2 removal from marine engine exhaust gas, *Energy Fuels*, 2007, **21**, 3274–3279.

34 E. Fridell and K. Salo, Measurements of abatement of particles and exhaust gases in a marine gas scrubber, *Proc. Inst. Mech. Eng. M: J. Eng. Marit. Environ.*, 2016, **230**, 154–162.

35 J. Zhou, S. Zhou and Y. Zhu, Characterization of Particle and Gaseous Emissions from Marine Diesel Engines with Different Fuels and Impact of After-Treatment Technology, *Energies*, 2017, **10**, 1110.

36 K. Lehtoranta, P. Aakko-Saksa, T. Murtonen, H. Vesala, L. Ntziachristos, T. Rönkkö, P. Karjalainen, N. Kuittinen and H. Timonen, Particulate Mass and Nonvolatile Particle Number Emissions from Marine Engines Using Low-Sulfur Fuels, Natural Gas, or Scrubbers, *Environ. Sci. Technol.*, 2019, **53**, 3315–3322.

37 H. Winnes, E. Fridell and J. Moldanová, Effects of Marine Exhaust Gas Scrubbers on Gas and Particle Emissions, *J. Mar. Sci. Eng.*, 2020, **8**, 299.

38 J. Yang, T. Tang, Y. Jiang, G. Karavalakis, T. D. Durbin, J. Wayne Miller, D. R. Cocker and K. C. Johnson, Controlling emissions from an ocean-going container vessel with a wet scrubber system, *Fuel*, 2021, **304**, 121323.

39 K. I. Lieke, T. Rosenørn, J. Pedersen, D. Larsson, J. Kling, K. Fuglsang and M. Bilde, Micro- and Nanostructural Characteristics of Particles Before and After an Exhaust Gas Recirculation System Scrubber, *Aerosol Sci. Technol.*, 2013, **47**, 1038–1046.

40 L. F. E. d. Santos, K. Salo and E. S. Thomson, Quantification and physical analysis of nanoparticle emissions from a marine engine using different fuels and a laboratory wet scrubber, *Environ. Sci.: Process. Impacts*, 2022, **24**, 1769–1781.

41 T. Yuan, H. Song, R. Wood, C. Wang, L. Oreopoulos, S. E. Platnick, S. von Hippel, K. Meyer, S. Light and E. Wilcox, Global reduction in ship-tracks from sulfur regulations for shipping fuel, *Sci. Adv.*, 2022, **8**, 1–9.

42 IVL Swedish Environmental Research Institute, *Scrubbers: Closing the Loop Activity 3 : Task 1 Air Emission Measurements (No. B 2318)*, IVL Swedish Environmental Research Institute Ltd., P.O Technical Report, December, 2018.

43 G. C. Roberts and A. Nenes, A continuous-flow streamwise thermal-gradient CCN chamber for atmospheric measurements, *Aerosol Sci. Technol.*, 2005, **39**, 206–221.

44 S. Lance, J. Medina, J. Smith and A. Nenes, Mapping the operation of the DMT continuous flow CCN counter, *Aerosol Sci. Technol.*, 2006, **40**, 242–254.

45 R. H. Moore and A. Nenes, Scanning flow CCN analysis – a method for fast measurements of CCN spectra, *Aerosol Sci. Technol.*, 2009, **43**, 1192–1207.

46 T. B. Kristensen, J. Falk, R. Lindgren, C. Andersen, V. B. Malmborg, A. C. Eriksson, K. Korhonen, R. L. Carvalho, C. Boman, J. Pagels and B. Svenningsson, Properties and emission factors of cloud condensation nuclei from biomass cookstoves – observations of a strong dependency on potassium content in the fuel, *Atmos. Chem. Phys.*, 2021, **21**, 8023–8044.

47 M. D. Petters and S. M. Kreidenweis, A single parameter representation of hygroscopic growth and cloud

condensation nucleus activity – Part 2: Including solubility, *Atmos. Chem. Phys.*, 2008, **8**, 6273–6279.

48 R. C. Moffet, A. V. Tivanski and M. K. Gilles, *Fundamentals and Applications in Aerosol Spectroscopy*, CRC Press; Taylor & Francis Group, Boca Raton, FL, 2011.

49 F. Mahrt, C. Marcolli, R. O. David, P. Grönquist, E. J. Barthazy Meier, U. Lohmann and Z. A. Kanji, Ice nucleation abilities of soot particles determined with the Horizontal Ice Nucleation Chamber, *Atmos. Chem. Phys.*, 2018, **18**, 13363–13392.

50 Hitchcock Group Homepage, **https://unicorn.mcmaster.ca/axis/aXis2000-IDLVM.html**, accessed on , 2022-01-28.

51 D. R. Tree and K. I. Svensson, Soot processes in compression ignition engines, *Prog. Energy Combust. Sci.*, 2007, **33**, 272–309.

52 E. Weingartner, H. Burtscher and U. Baltensperger, Hygroscopic properties of carbon and diesel soot particles, *Atmos. Environ.*, 1997, **31**, 2311–2327.

53 T. Tritscher, Z. Jurnyi, M. Martin, R. Chirico, M. Gysel, M. F. Heringa, P. F. Decarlo, B. Sierau, A. S. Prévt, E. Weingartner and U. Baltensperger, Changes of hygroscopicity and morphology during ageing of diesel soot, *Environ. Res. Lett.*, 2011, **6**, 034026.

54 R. C. Moffet, T. Henn, A. Laskin and M. K. Gilles, Automated Chemical Analysis of Internally Mixed Aerosol Particles Using X-ray Spectromicroscopy at the Carbon K-Edge, *Anal. Chem.*, 2010, **82**, 7906–7914.

55 T. C. Bond and R. W. Bergstrom, Light Absorption by Carbonaceous Particles: An Investigative Review, *Aerosol Sci. Technol.*, 2006, **40**, 27–67.

56 P. A. Alpert, R. Ciuraru, S. Rossignol, M. Passananti, L. Tinel, S. Perrier, Y. Dupart, S. S. Steimer, M. Ammann, D. J. Donaldson and C. George, Fatty Acid Surfactant Photochemistry Results in New Particle Formation, *Sci. Rep.*, 2017, **7**, 12693.

57 A. Braun, F. E. Huggins, N. Shah, Y. Chen, S. Wirick, S. B. Mun, C. Jacobsen and G. P. Huffman, Advantages of soft X-ray absorption over TEM-EELS for solid carbon studies – A comparative study on diesel soot with EELS and NEXAFS, *Carbon*, 2005, **43**, 117–124.

58 G. Sarret, J. Connan, M. Kasrai, G. M. Bancroft, A. Charrié-Duhaut, S. Lemoine, P. Adam, P. Albrecht and L. Eybert-Bérard, Chemical forms of sulfur in geological and archeological asphaltenes from Middle East, France, and Spain determined by sulfur K- and L-edge X-ray absorption near-edge structure spectroscopy, *Geochim. Cosmochim. Acta*, 1999, **63**, 3767–3779.

59 R. J. Hopkins, Y. Desyaterik, A. V. Tivanski, R. A. Zaveri, C. M. Berkowitz, T. Tyliszczak, M. K. Gilles and A. Laskin, Chemical speciation of sulfur in marine cloud droplets and particles: Analysis of individual particles from the marine boundary layer over the California current, *J. Geophys. Res.*, 2008, **113**, D04209.

60 R. D. Davis, S. Lance, J. A. Gordon, S. B. Ushijima and M. A. Tolbert, Contact efflorescence as a pathway for crystallization of atmospherically relevant particles, *Proc. Natl. Acad. Sci. U. S. A.*, 2015, **112**, 15815–15820.

61 G. P. Peters, T. B. Nilssen, L. Lindholt, M. S. Eide, S. Glomsrød, L. I. Eide and J. S. Fuglestvedt, Future emissions from shipping and petroleum activities in the Arctic, *Atmos. Chem. Phys.*, 2011, **11**, 5305–5320.

62 A. Possner, A. M. Ekman and U. Lohmann, Cloud response and feedback processes in stratiform mixed-phase clouds perturbed by ship exhaust, *Geophys. Res. Lett.*, 2017, **44**, 1964–1972.

63 S. R. Stephenson, W. Wang, C. S. Zender, H. Wang, S. J. Davis and P. J. Rasch, Climatic Responses to Future Trans-Arctic Shipping, *Geophys. Res. Lett.*, 2018, **45**, 9898–9908.

64 H. Morrison, G. De Boer, G. Feingold, J. Harrington, M. D. Shupe and K. Sulia, Resilience of persistent Arctic mixed-phase clouds, *Nat. Geosci.*, 2012, **5**, 11–17.

65 M. D. Petters, A. J. Prenni, S. M. Kreidenweis, P. J. DeMott, A. Matsunaga, Y. B. Lim and P. J. Ziemann, Chemical aging and the hydrophobic-to-hydrophilic conversion of carbonaceous aerosol, *Geophys. Res. Lett.*, 2006, **33**, L24806.

66 X. Kong, D. Castarède, E. S. Thomson, A. Boucly, L. Artiglia, M. Ammann, I. Gladich and J. B. C. Pettersson, A surface-promoted redox reaction occurs spontaneously on solvating inorganic aerosol surfaces, *Science*, 2021, **374**, 747–752.

67 I. Bulatovic, A. L. Igel, C. Leck, J. Heintzenberg, I. Riipinen and A. M. L. Ekman, The importance of Aitken mode aerosol particles for cloud sustenance in the summertime high Arctic – a simulation study supported by observational data, *Atmos. Chem. Phys.*, 2021, **21**, 3871–3897.

68 T. Mauritsen, J. Sedlar, M. Tjernström, C. Leck, M. Martin, M. Shupe, S. Sjogren, B. Sierau, P. O. Persson, I. M. Brooks and E. Swietlicki, An Arctic CCN-limited cloud-aerosol regime, *Atmos. Chem. Phys.*, 2011, **11**, 165–173.